Paper No. 16a

AEROELASTIC STABILITY OF TRIMMED HELICOPTER BLADES IN FORWARD FLIGHT

by

P. Friedmann and J. Shamie
Mechanics and Structures Department
School of Engineering and Applied Science
University of California
Los Angeles, California, 90024, U.S.A.

ABSTRACT

Equations for moderately large amplitude coupled flap-lag motion of a torsionally rigid hingeless elastic helicopter blade in forward flight are derived. Quasi-steady aerodynamic loads are considered and the effects of reversed flow are included. By using Galerkin's method the spatial dependence of the problem is eliminated and the equations are linearized about a time dependent equilibrium position determined from the trimmed equilibrium position of the rotor in forward flight. Two separate trim procedures are used to determine the time varying equilibrium position. In the first trim procedure the rotor is maintained at a fixed value of thrust coefficient with forward flight and horizontal and vertical force equilibrium is satisfied in addition to maintaining zero pitch and roll moments. This procedure simulates actual forward flight conditions. The second trim procedure maintains only zero pitch and roll moments simulating conditions under which a rotor would be tested in the wind tunnel.

The resulting linear system of equations with periodic coefficients is solved by using multivariable Floquet-Liapunov theory. The effects of both types of trim procedures on rotor blade stability boundaries are determined. Furthermore the effects of various important blade parameters on the aeroelastic stability boundaries in forward flight are determined.

1. Introduction

During recent years the helicopter industry has witnessed a growing acceptance of hingeless rotor systems used in conventional helicopters flying at relatively high speeds. Although a number of quite successful hingeless rotored helicopters have been built and are in service, the correct mathematical modeling of this complex aeroelastic problem, for the case of forward flight, is still an area of aeroelasticity in which a significant amount of additional fundamental research is needed.

Studies dealing with the effect of forward flight have been primarily devoted to the treatment of flapping instability [1-4]. These studies were aimed at understanding the effect of the parametric excitation, or periodic coefficients, in the equations of motion and at developing suitable numerical schemes for dealing with periodic systems. A complete treatment of the aeroelastic stability problem in forward flight was not attempted in these studies.

A number of studies dealing with the effect of forward flight on the coupled flap-lap stability problem have been also conducted [5-10]. Young's work [6], which represented a pioneering effort was somewhat controversial, while Hall's work [5], in which the coupled flap-lag problem was considered was inconclusive, although it served a very useful purpose in introducing multivariable Floquet theory to rotor dynamics. The coupled-flap-lag problem was also considered by Friedmann and Tong [7,8], their treatment was limited to low

Paper presented at the First European Rotorcraft and Powered Lift Aircraft Forum, University of Southampton, Southampton, England, September 22-24, 1975.

advance ratios and was aimed primarily at understanding the importance of the nonlinear terms, due to moderately large deflections, in the equations of motion.

A more realistic attempt at dealing with the coupled flap-lag problem at arbitrary advance ratios was made in References 9 and 10. In these studies an effecient numerical scheme for dealing with periodic systems was presented, and the effect of forward flight on the fully coupled flap-lag motions was explored.

The main defficiency of References 9 and 10 as well as the various other studies dealing with coupled flap-lag dynamics [5-8], or flapping dynamics [1,4] is due to the fact that the time dependent trim state of the complete rotor is decoupled from the aeroelastic stability problem.

The purpose of the present study is to remedy this situation by properly including the trim effects and the time varying equilibrium position in the formulation and the solutions of the coupled flap-lag aeroelastic stability problem in forward flight. While the formulation of the equations is quite general, two separate trim procedures are used to determine the equilibrium position of the rotor. The first trim procedure maintains the rotor trimmed at a fixed value of the thrust coefficient C_T, in this procedure both horizontal and vertical force equilibrium are satisfied and the pitching and rolling moments are kept at zero, simulating actual conditions in forward flight. The second trim procedure maintains only zero pitch and roll moment conditions on the rotor and represents therefore typical conditions under which a rotor would be tested in a wind tunnel.

The effects of both types of trim procedures on rotor blade stability are determined by comparing these results with those obtained in previous studies [9,10]. Furthermore, the effects of various important parameters such as flapwise and inplane stiffness, structural damping, Lock number and preconing on stability boundaries in forward flight are considered.

Finally it is important to emphasize that while the present treatment does not consider the complete coupled rotor fuselage aeroelastic problem, it goes significantly beyond single blade analyses which are available in the literature.

2. The Equtions of Motion

2.1 General

The present study is based upon a consistently derived set of nonlinear equations describing the coupled flap-lag motion of a contilevered rotor blade. The equations of motion will be first derived in partial differential, nonlinear form. Subsequently these equations are linearized about a time dependent equilibrium position determined from trim conditions of the rotor. Due to the complexity of the equations only a relatively brief presentation of their derivation will be given.

2.2 Basic Assumptions for the Aeroelastic Analysis

The goemetry of the problem is shown in Figs. 1 and 2. The following basic assumptions were used in deriving the equations of motion used for the treatment of the aeroelastic stability problem: (a) The blade is cantilevered at the hub, its feathering axis can be preconed by an angle β_p, the angle β_p is small. (b) The blade can bend in two directions normal to the elastic axis and is torsionally rigid. (c) The deflections of the blade are moderately small so that terms of $0(\mathscr{E}_D^2)$ can be neglected compared to one. (d) Two-dimensional quasi-steady aerodynamic strip theory is used, i.e. $C(k) = 1$, and apparent mass effect are neglected. (e) Reversed flow is included by using an approximate model for

reversed flow as described in References 9 and 10. (f) Uniform inflow over the disk of the rotor is assumed, and the time varying components of the inflow are neglected. (g) Stall and compressibility effects are neglected. (h) The rotor is trimmed according to various trim procedures described in the following sections. (i) Single blade aeroelastic analysis of an isolated rotor blade attached to an aircraft of infinite mass is used. (j) The blade is assumed to have no pretwist. (k) Blade cross sectional center of gravity, elastic axis and aerodynamic center are coincident. (ℓ) Structural damping forces are assumed to be of a viscous type.

2.3 The Ordering Scheme

The present study is aimed at deriving first a set of nonlinear equations which will be subsequently linearized. In this process one encounters a considerable number of terms which are small and therefore negligible. In order to neglect the appropriate terms a rational ordering scheme is used which enables one to neglect terms in a systematic manner. In this scheme all the important parameters of the problems are assigned orders of magnitude in terms of a typical displacement quantity, $\mathscr{E}_D$, thus:

$$\frac{v}{\ell} = O(\mathscr{E}_D) \quad ; \quad \frac{w}{\ell} = O(\mathscr{E}_D) \quad , \quad \frac{x}{R} = O(1)$$

$$\theta_o = O(\mathscr{E}_D^{1/2}); \quad \theta_{1s} = O(\mathscr{E}_D) \quad ; \quad \theta_{1c} = O(\mathscr{E}_D)$$

$$\lambda = O(\mathscr{E}_D) \quad ; \quad \frac{\partial w}{\partial x_o} = \frac{\partial v}{\partial x_o} = O(\mathscr{E}_D) \quad ;$$

$$\beta_p = O(\mathscr{E}_D) \quad ; \quad C_{do}/a = O(\mathscr{E}_D^{3/2}) \quad ; \quad b = O(\mathscr{E}_D)$$

$$\mu = O(1).$$

This ordering scheme together with assumption (c) of the previous section implies that terms of $O(\mathscr{E}_D^2)$ are neglected compared to terms of O(1) in the equations of motion. Obviously the ordering scheme should be used with a certain degree of flexibility and physical insight so as to enable one to retain certain higher order terms of importance even though they may appear negligible when considered strictly in the light of the ordering scheme.

2.4 Brief Derivation of the Blade Equations of Motion

Using the assumptions and the ordering scheme given above a system of nonlinear partial differential equations for the coupled flap-lag motion of the blade is derived, with respect to a x,y and z coordinate system rotating with the blade. The derivation of the inertia and aerodynamic operators of this aeroelastic problem follows essentially along the lines of References 7,10,11 which the derivation of the structural operator is essentially similar to the one presented in Houbolt and Brooks [12].

Thus the differential equation for the dynamic equilibrium of the blade can be written as [11,12],

$$\frac{\partial^2}{\partial x_o^2}\left\{[(EI)_y + E_{c1}]\frac{\partial^2 w_e}{\partial x_o^2} + E_{c2}\frac{\partial^2 v_e}{\partial x_o^2}\right\} - \frac{\partial}{\partial x_o}\left[T\frac{\partial w}{\partial x_o}\right] = p_z$$

$$\frac{\partial^2}{\partial x_o^2}\left\{[(EI)_z - E_{c1}]\frac{\partial^2 v_e}{\partial x_o^2} + E_{c2}\frac{\partial^2 w_e}{\partial x_o^2}\right\} - \frac{\partial}{\partial x_o}\left[T\frac{\partial v}{\partial x_o}\right] = p_y \qquad (1)$$

where the quantities

$$E_{c1} = [(EI)_z - (EI)_y] \sin^2(\theta_o + \theta_t)$$
$$E_{c2} = [(EI)_z - (EI)_y] \sin(\theta_o + \theta_t)\cos(\theta_o + \theta_t) \tag{2}$$

represent elastic coupling terms due to the collective pitch setting θ_o and the cyclic pitch

$$\theta_t = \theta_{1c} \cos\psi + \theta_{1s} \sin\psi \quad . \tag{3}$$

A list of symbols is given in Appendix D.

The distributed loading terms in Equations (1) representing the combined general aerodynamic, inertial and structural damping loads for this aeroelastic problem can be written as [10,11]

$$P_x = -\frac{\partial T}{\partial x_o} = m\Omega^2[(x_o + e_1) + 2\overset{*}{v}] \tag{4}$$

$$P_y = L_{Y2} - m\Omega^2[\overset{**}{v} - (e_1 + v) + 2\overset{*}{u}] - g_{SL}\Omega\overset{*}{v}_e \tag{5}$$

$$P_z = L_{Z2} - m\Omega^2 \overset{**}{w} - g_{SF}\Omega\overset{*}{w}_e \quad . \tag{6}$$

The aerodynamic loads L_{Z2} and L_{Y2} in the z and y directions respectively, are given by [10,11]

$$L_{Z2} = \rho_A abR\left[U_{Y2}^2(\theta_o + \theta_t) - U_{Z2}U_{Y2} - (3/2)U_{Y2}bR\Omega\,\overset{*}{\theta}_t\right] \tag{7}$$

$$L_{Y2} = -\rho_A abR\left[(\theta_o + \theta_t)U_{Z2}U_{Y2} - U_{Z2}^2 + \frac{C_{do}}{a}U_{Y2}^2 - 1.5U_{Z2}bR\Omega\,\overset{*}{\theta}_t\right]. \tag{8}$$

Where the velocity components U_{Y2} and U_{Z2} are given by

$$-U_{Y2} \cong U_T = \Omega\overset{*}{v} + \Omega(x_o + e_1) + \Omega R\mu\left[\sin\psi + \cos\psi\,\frac{\partial v}{\partial x_o}\right] \tag{9}$$

$$-U_{Z2} \cong U_P = \Omega\left[\overset{*}{w} + R\lambda + v\,\frac{\partial w}{\partial x_o} + R\mu\,\cos\psi\,\frac{\partial w}{\partial x_o}\right] \quad . \tag{10}$$

The last ingredient required to formulate this aeroelastic problem is the displacement field for a point on the elastic axis of the blade given by

$$u = -\beta_p w_e - \frac{x_o}{2}\beta_p^2 - \frac{1}{2}\int_o^{x_o}\left[\left(\frac{\partial w_e}{\partial x_1}\right)^2 + \left(\frac{\partial v_e}{\partial x_1}\right)^2\right]dx_1 \tag{11}$$

$$v = v_e \tag{12}$$

$$w = w_e + \beta_p\, x_o \tag{13}$$

The boundary conditions for this set of partial differential equations are:

$$\text{at } x_o = 0 \quad . \quad v_e = w_e = \frac{\partial v_e}{\partial x_o} = \frac{\partial w_e}{\partial x_o} = 0$$

while at $x_o = \ell$ the shears and moments are zero.

The system of general, coupled, partial differential equations of motion presented in Equations (1) through (13) above is transformed into a system of ordinary nonlinear differential equations by using Galerkin's method to eliminate the spatial variable. In this process the elastic degrees of freedom in the problem are represented by the uncoupled free vibration modes of a rotating blade. The present study is restricted to the case of a single elastic mode representing each elastic degree of freedom. The modal representation of the elastic degrees of freedom is given by

$$\begin{aligned} w_e &= \ell\, \eta_1(\overline{x_o})\, g_1(\psi) \\ v_e &= -\ell\gamma_1(\overline{x_o})\, h_1(\psi) \end{aligned} \qquad . \tag{14}$$

The ordinary nonlinear differential equations are given by

$$\begin{aligned} &\bar{M}_{F1}\overset{**}{g}_1 + 2\bar{\omega}_{F1}\, M_{F1}\eta_{SF1}\overset{*}{g}_1 + \bar{M}_{F1}\bar{\omega}^2_{F1} g_1 + \beta_p\overline{B^1} + g_1\bar{E} - \\ &\quad - \cos 2\theta_t(\overline{E^c}\, g_1 + \bar{E}^{1s} h_1) + \sin 2\theta_t(g_1\overline{E^s} - h_1\bar{E}^{1c}) \\ &\quad - 2\beta_p\overline{B^2}\,\overset{*}{h}_1 - 2g_1\overset{*}{h}_1\,\bar{P}_{111} = A_{F1} \end{aligned} \tag{15}$$

$$\begin{aligned} &\bar{M}_{L1}\overset{**}{h}_1 + 2\bar{\omega}_{L1}M_{L1}\eta_{SL1}\,\overset{*}{h}_1 + \bar{M}_{L1}\bar{\omega}^2_{L1}h_1 - \cos 2\theta_t(g_1\bar{\bar{E}}^{1s} - \bar{\bar{E}}^c h_1) \\ &- h_1\bar{\bar{E}} - \sin 2\theta_t(\bar{\bar{E}}^{1c} g_1 + \bar{\bar{E}}^s h_1) + 2\bar{M}_{111}g_1\overset{*}{g}_1 + 2\beta_p\bar{\bar{B}}^2\overset{*}{g}_1 = A_{L1} \end{aligned} \tag{16}$$

where the various quantities $\bar{M}_{F1}$, $\bar{M}_{L1}$,...$\bar{P}_{111}$,...$\bar{E}$,...etc. are defined in Appendix A and A_{F1} and A_{L1} are the generalized aerodynamic loads for flap and lag respectively given by

$$A_{F1} = \ell^2 \int_{\bar{A}}^{\bar{B}} L_{Z2}\eta_1\, d\bar{x}_o/\Omega^2 I_b \tag{17}$$

$$A_{L1} = -\ell^2 \int_{\bar{A}}^{\bar{B}} L_{Y2}\gamma_1\, d\bar{x}_o/\Omega^2 I_b \quad . \tag{18}$$

3. The Trim Procedures

3.1 General

In this study the nonlinear equations of motions developed in the previous sections, will be linearized about a time dependent equilibrium position which is determined from the trimmed equilibrium position of the helicopter in forward flight. In the first trim procedure the rotor is maintained at a fixed value of thrust coefficient with forward flight and horizontal and vertical force equilibrium is satisfied in addition to maintaining zero pitch and roll moments. This procedure simulates actual forward flight conditions.

In the second trim procedure only zero pitching and rolling moments on the rotor are maintained simulating conditions under which a rotor would be tested in the wind tunnel.

3.2 Assumptions for the Trim Procedure

In order to construct trim procedures for the aeroelastic stability problem care should be exercised so as to have a realistic representation which would provide physically meaningful results. On the other hand some simplifying assumptions have to be made otherwise the trim problem by itself can become quite complicated [13]. These simplifying assumptions are presented below: (a) The helicopter is in straight and level steady flight ($\gamma_F = 0$, see Fig. 3). (b) Pitching and rolling moments on the rotor are equal to zero. (c) Flapping response of the trimmed rotor is assumed to consist completely of the first or fundamental mode in flapping, i.e. effect of the lead-lag degree of freedom on the trim state of the rotor is neglected. Furthermore only first harmonics are considered, higher harmonics are neglected. (d) The rotor hub and helicopter center of gravity coincide, i.e. the whole aircraft is represented by a point mass coinciding with the hub. (e) Tail, fuselage moments and side force components are neglected. (f) Effect of precone and reversed flow on the trim state is neglected. (g) Effect of Coriolis terms is neglected. (i) The total geometric pitch angle is assumed to be given by

$$\theta_G = \theta_o + \theta_{1s}\sin\psi + \theta_{1c}\cos\psi \quad . \tag{19}$$

(j) Various forces used are considered to be average forces over one revolution and the first mode flapping response is given by

$$g_1 = \tilde{g}_1^o + \tilde{g}_{1s}\sin\psi + \tilde{g}_{1c}\cos\psi \quad . \tag{20}$$

3.3 Brief Derivation of the Equations for the Trim Procedures

Using the geometry shown in Fig. 3 together with the assumptions given above, the requirement of force equilibrium tangential and normal to the flight path (for $\gamma_F = 0$ this is identical to horizontal and vertical force equilibrium) as well as pitching and rolling moment equilibrium results in the following equations

$$m_T \dot{V} = 0 = -T\sin\alpha_R + H\cos\alpha_R + D_P \tag{21}$$

$$T\cos\alpha_R = m_T g \tag{22}$$

$$(M_{pa})_R = 0 \tag{23}$$

$$(M_{ra})_R = 0 \quad . \tag{24}$$

It is more convenient to rewrite Equation (21) in nondimensional form

$$-C_T\sin\alpha_R + C_H\cos\alpha_R + \frac{1}{2}C_{DP}\frac{\mu^2}{\cos^2\alpha_R} = 0 \quad . \tag{25}$$

Using Equations (22) through (25) the trim state of the rotor can be obtained [7,13] provided that appropriate expressions for the thrust coefficient C_T, horizontal force coefficient C_H and blade root moment M_R are first obtained.

In order to calculate the pitching and rolling moment, an expression for the root flapping moment, shown in Fig. 4, is required. Neglecting Coriolis

forces the moment at the blade root due to aerodynamic, centrifugal and inertia forces is given by (for $\ell = R$, $e_1 = 0$, and $\beta_p = 0$)

$$M_R(0,\psi) = \int_0^{\ell} \left[L_{Z2} - m\Omega^2 \frac{\partial^2 w_e}{\partial \psi^2} - m\Omega^2 w_e \right] x_o dx_o \quad . \tag{26}$$

The uncoupled equation of bending equilibrium in the flap direction yields

$$\frac{\partial^2}{\partial x_o^2} \left[(EI)_y \frac{\partial^2 w_e}{\partial x_o^2} \right] - \frac{\partial}{\partial x_o} \left(T \frac{\partial w}{\partial x_o} \right) + m \frac{\partial^2 w}{\partial t^2} = L_{Z2} \quad . \tag{27}$$

Using the first elastic mode shape equation (14) and combining Equations (26) and (27) yields

$$M_R(0, \ ) = \ell \int_0^{\ell} \left\{ \frac{d^2}{dx_o^2} \left[(EI)_y \frac{d^2 \eta_1}{dx_o^2} \right] - \frac{d}{dx_o} \left(T \frac{d\eta_1}{dx_o} \right) - m\Omega^2 \eta_1 \right\} g_1 x_o dx_o \quad . \tag{28}$$

From the free vibration problem of a rotating beam

$$\frac{d^2}{dx_o^2} \left[(EI)_y \frac{d^2 \eta_1}{dx_o^2} \right] - \frac{d}{dx_o} \left(T \frac{d\eta_1}{dx_o} \right) = m\bar{\omega}_{F1}^2 \Omega^2 \eta_1 \quad . \tag{29}$$

Combining the last two equations with Equation (20) the required root moment expression is obtained

$$M_R(0,\psi) = \ell^3 \Omega^2 (\bar{\omega}_{F1}^2 - 1)(\tilde{g}_1^o + \tilde{g}_{1c} \cos\psi + \tilde{g}_{1s} \sin\psi) \int_0^1 m\bar{x}_o \eta_1 d\bar{x}_o \tag{30}$$

Pitching and rolling moments for a single blade are obtained by a simple vector decomposition of $M_R(0,\psi)$ shown in Fig. 4

$$M_p = M_R(0,\psi)\cos\psi \tag{31}$$

$$M_r = M_R(0,\psi)\sin\psi \quad . \tag{32}$$

For trim purposes, the average values of these quantities, per revolution, are required. Combining Equations (30) through (32)

$$M_{pa} = \frac{1}{2\pi} \int_0^{2\pi} M_R(0,\psi)\cos\psi d\psi = \frac{1}{2}(\bar{\omega}_{F1}^2 - 1)\ell^3 \Omega^2 \tilde{g}_{1c} \int_0^1 m\bar{x}_o \eta_1 d\bar{x}_o \tag{33}$$

$$M_{ra} = \frac{1}{2\pi} \int_0^{2\pi} M_R(0,\psi)\sin\psi d\psi = \frac{1}{2}(\bar{\omega}_{FL}^2 - 1)\ell^3 \Omega^2 \tilde{g}_{1s} \int_0^1 m\bar{x}_o \eta_1 d\bar{x}_o \quad . \tag{34}$$

For an n_b bladed rotor the average pitching and rolling moment for the complete rotor will be given by

$$(M_{pa})_R = M_{pa} n_b \quad \text{and} \quad (M_{ra})_R = M_{ra} n_b \quad .$$

From Equations (23), (24), (33) and (34), it is clear that for pitching and rolling moment equilibrium

$$\tilde{g}_{1c} = \tilde{g}_{1s} = 0 \quad . \tag{35}$$

The thrust coefficient of a hingeless blade can be obtained by using the assumptions presented in Section 3.2. Neglecting nonlinear terms and using uniform inflow over the rotor disk given by

$$\lambda = \mu \tan\alpha_R + \frac{C_T}{2\sqrt{\mu^2 + \lambda^2}} \quad . \tag{36}$$

The expressions for U_P and U_T can be written as

$$U_P = (\lambda + \mu\eta_1' g_1 \cos\psi + \ell\, \eta_1 \overset{*}{g}_1/R)\Omega R \tag{37}$$

$$U_T = \Omega R(\mu\sin\psi + \bar{x}) \quad . \tag{38}$$

The average value of the thrust coefficient defined as

$$C_T = \frac{T}{\rho_A(\pi R^2)(\Omega R)^2} = \frac{n_b}{2\pi\rho_A(\pi R^2)(\Omega R)^2} \int_0^{2\pi}\int_{\bar{A}}^{\bar{B}} L_{Z2}\,\ell\, d\bar{x}d\psi \tag{39}$$

is given by

$$C_T = \frac{\sigma\cdot a}{2}\left(\frac{\ell}{R}\right)\left[\theta_o(F^{18} + \frac{1}{2}\mu^2 F^{21}) - F^{17}\lambda + \mu F^{17}\theta_{1s}\right] \quad . \tag{40}$$

The horizontal force component per unit span is given by the following relation [7,13]

$$\frac{dH}{dx_o} = - L_{Y2}\sin\psi - L_{Z2}\frac{\partial w}{\partial x_o}\cos\psi \tag{41}$$

where

$$\phi \cong U_P/U_T \quad .$$

Using Equations (37), (38), (7), (8) and (41) the average horizontal force is given by

$$H = \frac{n_b(bR)\rho_A\ell}{2\pi}\int_{\bar{A}}^{\bar{B}}\int_o^{2\pi}\Big\{[U_T^2 C_{do} + a(U_P U_T\theta_G - U_P^2)]\sin\psi d\bar{x}_o d\psi$$

$$- a(\theta_G U_T^2 - U_P U_T) g_1\eta_1' \cos\psi d\bar{x}_o d\psi\Big\} \tag{42}$$

from which

$$C_H = 0.5\, C_{do}\mu\sigma F^{17}(\ell/R) + (\sigma\cdot a/4)(\ell/R)[\theta_o\lambda\mu F^{21} + \theta_{1s}\lambda F^{17}]$$

$$- (\sigma a/4)(\ell/R)\tilde{g}_1^o(F^{19}\theta_{1c} - \mu\tilde{g}_1^o F^{20}) \quad . \tag{43}$$

The last ingredient required for the calculation of the trim state of the rotor are the so called flapping coefficients. Neglecting Coriolis forces, structural damping and nonlinear terms the flapping coefficients are obtained from the steady state solution of the flapping equation

$$\bar{M}_{F1}\ddot{g}_1^{**} + \bar{M}_{F1}\,\bar{\omega}_{F1}^2\, g_1 = \frac{\gamma}{2}\left(\frac{\ell}{R}\right)^2 \int_{\bar{A}}^{\bar{B}} L_{Z2}\eta_1 d\bar{x}_o = A_{F1} \quad . \tag{44}$$

Using uniform inflow λ and neglecting higher harmonic terms in the calculation of the flapping coefficients, one has

$$A_{F1} = \frac{\gamma}{2}\left(\frac{\ell}{R}\right)^2 [F^1\theta - F^2\lambda + F^3\theta\,\frac{\mu^3}{2} + \mu(2\theta F^2 - \lambda F^3)\sin\psi$$
$$- \mu\, F^6 g_1\cos\psi - (\ell/R)(F^8 + F^9\mu\sin\psi)\ddot{g}_1^{*}] \tag{45}$$

Substituting Equations (19), (20), and (35) into (44) and (45), and collecting the constant terms, the terms multiplied by $\cos\psi$ and the terms multiplied by $\sin\psi$ one obtains the three flapping equations given below.

$$\bar{\omega}_{F1}^2\tilde{g}_1^{o} - \frac{\gamma}{2}\left(\frac{\ell}{R}\right)^2 \frac{1}{\bar{M}_{F1}}[\theta_o(F^1 + \tfrac{1}{2}F^3\mu^2) - F^2\lambda + \mu F^2\theta_{1s}] = 0 \tag{46}$$

$$(F^1 + F^3\mu^2/4)\theta_{1c} - \mu\tilde{g}_1^{o}\, F^6 = 0 \tag{47}$$

$$(F^1 + 3F^3\mu^2/4)\theta_{1s} + 2\mu\theta_o F^2 - \mu\lambda F^3 = 0 \tag{48}$$

Solving these equations one obtains

$$\theta_{1s} = (\mu\lambda F^3 - 2\mu\theta_o F^2)/(F^1 + 3F^3\mu^2/4) \tag{49}$$

$$\tilde{g}_1^{o} = b_1\theta_o + b_2\lambda \tag{50}$$

$$\theta_{1c} = \mu\tilde{g}_1^{o}F^6/(F^1 + F^3\mu^2/4) \tag{51}$$

Where the various quantities F^i, $\bar{M}_{F1}\ldots b_1, b_2\ldots$etc. are defined in Appendix A.

3.4 The Trim Procedures

Using the equations presented in the previous section two separate trim procedures are developed.

(a) Propulsive Trim. In this trim procedure, which simulates actual forward flight conditions, the rotor is maintained at a fixed value of the thrust coefficient C_T with forward flight and the horizontal and vertical force equilibrium is maintained as required by Equations (21) and (22). Furthermore zero pitching and rolling moments on the rotor are also maintained.

The trim state is evaluated in the following manner: (1) The flight condition as determined by μ and C_T is given. (2) The value of the inflow is evaluated from Equation (36) for an arbitrary value of α_R. (3) The value of collective pitch θ_o is evaluated from Equations (40) and (49) for an arbitrary value of α_R. (4) $\tilde{g}_1^{o}$ and θ_{1c} are evaluated from Equations (50) and (51) for an arbitary

value of α_R. (5) Combining Equations (25) and (43) α_R is iterated upon until Equation (25) is satisfied and α_R for the trim state is obtained. (6) Using this value of α_R the quantities λ, θ_o, θ_{1s}, θ_{1c} and $\tilde{g}_1^o$ are obtained from the appropriate equations.

(b) Wind Tunnel Trim or Moment Trim in this trim procedure, which simulates conditions under which a rotor would be tested in the wind tunnel, pitching and rolling moments on the rotor are maintained at zero. Horizontal and vertical force equilibrium is not required for this case because the rotor is mounted on a supporting structure.

For this case the trim state is obtained in the following manner: (1) The test condition is specified by given values of μ, θ_o and α_R. (2) The inflow λ is evaluated from Equation (36) for an arbitrary value of C_T. (3) θ_{1s} is calculated from Equation (49) for an arbitrary value of C_T. (4) The thrust coefficient is iterated upon until Equation (40) is satisfied, thus the thrust coefficient for the trim state is determined. (5) Using this value of C_T the quantities λ, θ_{1s}, θ_{1c} and $\tilde{g}_1^o$ are determined from the appropriate equations.

4. Linearized Modal Equations of Motion

4.1 The Time Dependent Equilibrium Position of the Blade

The time dependent equilibrium position about which the equations of motion are linearized is a result of the cyclic pitch variation required to trim the rotor in forward flight. These cyclic pitch components are obtained from the trim procedures which have been described in the previous section.

The time dependent equilibrium position of blade can be determined from various considerations. In order to keep this process reasonably simple two assumptions will be made, these are:

(a) In the calculation of the time dependent equilibrium position only first harmonic terms, i.e. $\sin\psi$ and $\cos\psi$ terms will be considered. Thus the time dependent equilibrium position of the blade is written as

$$\bar{g}_1(\psi) = g_1^o + g_{1c}\cos\psi + g_{1s}\sin\psi \tag{52}$$

$$\bar{h}_1(\psi) = h_1^o + h_{1c}\cos\psi + h_{1s}\sin\psi \tag{53}$$

(b) An approximate linear time dependent equilibrium position is defined by neglecting combinations of the type: $g_1^o h_{1s}$, $g_1^o h_{1c}$, $g_1^o g_{1c}$, $g_1^o g_{1s}$, $h_1^o h_{1s}$, $h_1^o h_{1c}$, $h_1^o g_{1c}$, $h_1^o g_{1s}$, $h_{1c} g_{1c}$, $h_{1c} g_{1s}$,...etc. which are nonlinear combinations of the terms defining the equilibrium position. A more complete treatment which includes these terms will be presented elsewhere.

Using these assumptions and substituting Equations (19), (52) and (53) into Equations (15) and (16) the quantities g_1^o, g_{1c}, g_{1s}, h_1^o, h_{1c} and h_{1s} are obtained by requiring that the constant terms, $\cos\psi$-terms and $\sin\psi$-terms be equal to zero. After a considerable amount of algebraic manipulation this simple harmonic balancing results in a system of six linear algebraic equations for the unknowns, which can be written as

$$[S]\{q_o\} = \{C\} \tag{54}$$

where $\{q_o\}^T = \lfloor g_1^o\ g_{1c}\ g_{1s}\ h_1^o\ h_{1c}\ h_{1s} \rfloor$ and the elements S_{ij} and C_i of the appropriate matrices are given in Appendix B. The time dependent equilibrium position is obtained from

$$\{q_o\} = [S]^{-1} \{C\} \tag{55}$$

It is worth mentioning that Equations (55) are solved for both the normal and the reversed flow regions.

4.2 The Linearized Equations

The process of linearization of the equations of motion consists of expressing the elastic part of the displacement field as

$$\begin{aligned} w_e &= w_{eo} + \Delta w_e = \eta_1(\bar{g}_1 + \Delta g_1) \\ v_e &= v_{eo} + \Delta v_e = \gamma_1(\bar{h}_1 + \Delta h_1) \ . \end{aligned} \tag{56}$$

Equations (56) are substituted into Equations (15) and (16), in this process nonlinear terms are transformed into coupling terms, while terms of type $\Delta g_1 \Delta h_1$, $(\Delta g_1)^2$, $(\Delta h_1)^2$ are neglected.

Furthermore for mathematical convenience the equations of motion are transformed into first order state variable form by using the following notation

$$\Delta \overset{*}{g}_1 = y_1 \ ; \quad \Delta \overset{*}{h}_1 = y_3 \ ; \quad \Delta g_1 = y_2 \ ; \quad \Delta h_1 = y_4 \ . \tag{57}$$

For the determination of the aeroelastic stability boundaries only the homogeneous part of the equations of motion is required; thus the equations of motion in their final form are written as

$$\{\overset{*}{y}\} = [A(\psi)] \{y\} \tag{58}$$

where [A] is a 4×4 matrix defined in Appendix C.

The equations of motion (58) will have different forms, respectively, for the normal flow region and for the reversed flow region. The representation of the reversed flow together with its effect on the form of Equations (58) is described in Reference 10.

5. Method of Solution

The stability investigation of the blade motions is based upon the Floquet-Liapunov theorem [14] which states that the knowledge of the state transition matrix over one period is sufficient in order to determine the stability of a periodic system having a common period, T. Based upon the Floquet-Liapunov theorem, the transition matrix for the periodic system can be written as [14]

$$[\Phi(\psi,\psi_o)] = [P^{-1}(\psi)] e^{[R](\psi-\psi_o)} [P(\psi_o)] \tag{59}$$

where the $[P(\psi)]$ matrix is also periodic and [R] is a constant matrix. The stability of the system is governed by the matrix [R], where [R] is given by

$$[\Phi(T,0)] = e^{[R]T} = [C] \tag{60}$$

The stability for the system is related to the characteristic exponents or the eigenvalues of [R] denoted by

$$\lambda_k = \zeta_k + i\omega_k \tag{60}$$

The solutions of Equations (58) approach zero as $\psi \to \infty$ if

$$\zeta_k < 0, \qquad k = 1,2,\ldots n \tag{62}$$

The key to the efficient numerical treatment of periodic systems is the numerical computation of the transition matrix at the end on one period [$\Phi(T,0)$]. In the present study the transition matrix at the end of the period was obtained using a generalization of the rectangular ripple method described in Reference 9. The eigenvalues of [$\Phi(T,0]$ were evaluated using a Jacobi type eigenvalue routine.

6. Results and Discussion

6.1 Numerical Quantities Used in the Calculations

In the computation of the numerical results it was assumed that the mass and stiffness distributions are constant along the span of the blade. Rotating mode shapes for the flap and lag degrees of freedom were obtained by using Galerkin's method based upon five nonrotating cantilever mode shapes for each flap or lag degree of freedom. A convenient plot relating rotating and nonrotating frequencies can be found in Reference 10. The various spanwise integrations were performed using seven point Gaussian integration.

For cases dealing with linearization about the static equilibrium position in hover [10] the inflow was evaluated from

$$\lambda = (a\sigma/16)[(1 + 24\theta/a\sigma)^{1/2} - 1] \quad . \tag{63}$$

This relation was also used for calculating the inflow at $\mu = 0$ in the wind tunnel trim or moment trim procedure.

Finally, in all cases the following values were used:

$$Cd_o = 0.01; \quad a = 2\pi; \quad \sigma = 0.05; \quad C_{DP} = 0.01; \quad e_1 = 0;$$

$$\bar{A} = 0; \quad \bar{B} = 1.0 \quad ; b = 0.0313 \; .$$

Various other pertinent quantities are specified on the plots. Reversed flow was included in the calculation using the method described in Reference 10.

6.2 Results

The results presented in this study include the effects of reversed flow which is treated using a very convenient reversed flow model described in Reference 10.

As stated in the introduction, this study is primarily aimed at determining the effects of various trim procedures on the coupled flap-lag aeroelastic stability boundaries of a single blade. The physical meaning of the two trim procedures used in this study are best illustrated by trim curves showing the values of the various parameters associated with each trim procedure. The trim curves shown in Fig. 5 were obtained using the propulsive trim procedure for $C_T = 0.005$. These curves are shown for values of advance ratios up to $\mu = 0.40$ because above this value the propulsive trim equations cannot be satisfied anymore with $C_{DP} = 0.01$. The range of μ for this type of trim procedure can be stretched by increasing C_T or by employing two correction factors, denoted by CDPFAC and CDZFAC respectively, to multiply C_{DP} and C_{do}. Where it is understood that these correction factors can vary between $0 \div 1.0$. These correction factors enable one to simulate approximately the unloading of the rotor at high speeds. Trim curves obtained using the wind tunnel or moment trim procedure are shown in

Fig. 6; for $\alpha_R = 0.0$ and $\theta = 0.15$. Comparing Figs. 5 and 6, it is clear that the moment trim procedure is characterized by significant variations in the thrust coefficient C_T. While the curves for θ_{1s} and θ_{1c} are somewhat similar in both cases, the curves for θ_o and C_T are significantly different. Thus it is clear that the trim procedure used can significantly affect the aeroelastic stability boundaries.

It is pointed out in Reference 10 that the underlined term in Equation (10) was not included in the calculations. It seems reasonable therefore to determine the sensitivity of previous results, which were obtained by linearizing the equations of motion about the static equilibrium position in hover [10], to the missing term. The results for a typical case were recomputed here with and without this term. The results shown in Fig. 7 indicate that the missing term is destabilizing and reduces the value of μ_c for this particular case by approximately $\sim 21\%$. All the results in this study include the effect of this term.

The effects of the propulsive trim procedure on a typical case, considered in Reference 10, are shown in Fig. 8. Compared to the previous procedure [10], of linearizing the equations of motion about the linear equilibrium position in hover, the new results which account for the propulsive trim and the time dependent equilibrium position indicate that this, more realistic model of the blade dynamics, produces a more stable system. The results are presented only in the range $0 < \mu < 0.5$, outside this range the blade cannot be trimmed. From this Figure it is clear that the amount of damping in the lead-lag degree of freedom is significantly increased due to the effects associated with propulsive trim.

The combined effect of the trim procedures and the lock number on blade stability is illustrated by Figs. 9 and 10. Figure 9 illustrates the effect of both propulsive and moment trim at a low value of $\gamma(\gamma = 5)$ for a case for which the various parameters are specified on the plot. For this case a relatively high value of C_T was chosen ($C_T = 0.01$), so that the range of validity of propulsive trim could be stretched to $\mu = 0.6$. The figure shows that the blade did not become unstable in this range of μ's. The figure indicates that up to $\mu=0.4$ the real part of the characteristic exponents for both flap and lag behave in a similar manner for both trim procedures. When using the moment trim procedure the blade becomes unstable at $\mu_c = 0.90$ and the degree of freedom associated with the instability is the flap degree of freedom. The instability occurs at a nondimensional frequency of 0 (or 1) indicating that parametric excitation due to the periodic coefficients is the mechanism inducing the instability. Similar results are shown in Fig. 10 where the real part of the characteristic exponent associated with the lead-lag degree of freedom is plotted. Three separate cases are shown. For the first case, which is linearized about the static equilibrium position in hover [10], the lag degree of freedom becomes unstable at $\mu_c = 0.275$ with $\omega_k = 1.4705$. In the second case the propulsive trim procedure is used for this case the system is significantly more stable but the trim procedure cannot be used above $\mu = 0.55$. In the last case moment trim is used and the system becomes unstable at $\mu_c = 0.80$ and again the lag degree of freedom is the unstable one, the frequency of this instability is $\omega_k = 1.6555$ but the other frequencies associated with the flap degree of freedom in the vicinity of this point indicate significant coupling with the parametric excitation.

The sensitivity of the results, obtained from the moment trim procedure, to the rotor shaft angle α_R is illustrated by Fig. 11. Where a typical case is evaluated with two different values of α_R. The results indicate a relative insensitivity to this parameter. The same case was also evaluated with moment trim and a different value of the angle of precone. The results shown in Fig. 12 indicate that the results are not significantly affected by an angle of precone of 2°. Various other cases computed with precone indicated a similar insensitivity to precone except for lead-lag rotating frequencies in the vicinity of 1.

Results indicating the effect of forward flight on a soft inplane rotor are presented in Fig. 13. The results with moment trim indicate that the collective pitch setting can significantly influence blade stability. By increasing the collective pitch setting from $\theta = .15$ to $\theta = .30$ the value of the critical advance ratio at which the blade becomes unstable is reduced from $\mu_c = 0.86$ to $\mu_c = 0.19$.

Figure 14 illustrates the effect of the moment trim procedure on blade stability. When linearizing the equations about the linear equilibrium position in hover [10] the blade becomes unstable at $\mu_c = 0.27$. Linearization of the equations about the equilibrium position determined from moment trim increases the value of μ_c to $\mu_c = 0.48$.

Similar cases were computed for $\bar{\omega}_{F1} = 1.1006$ and $\bar{\omega}_{L1} = 0.7941$ with $\gamma = 10$, and $\theta = 0.15 \div 0.30$. The results indicate similar trends and therefore are not presented here.

All the results obtained in this study indicate that when the blade equations are linearized about the static equilibrium position in hover [10] the blade becomes unstable at a lower value of μ_c than when the equations are linearized about the time dependent equilibrium position determined from the propulsive trim or the moment trim procedure. This indicates that the results for the stability boundaries obtained in References 9 and 10 can be considered to be conservative.

7. Conclusions

The major conclusions obtained from the present study are summarized below. They should be considered indicative of trends and their application to the design of a helicopter rotor should be limited by the various assumptions which have been used.

(1) The two trim procedures developed and used in this study have a very significant effect on the coupled flap-lag aeroelastic stability boundaries in forward flight. In general, the amount of damping in the lead-lag mode is increased when the trim state is coupled with the aeroelastic system. The effect of the trim state influences blade stability through changes in collective pitch, inflow and the time dependent elastic coupling effect associated with the cyclic pitch components θ_{1c} and θ_{1s}.

(2) The relatively limited number of cases considered in this study seem to indicate that forward flight tends to destabilize the soft inplane hingeless blade to a greater degree than it affects the stiff inplane blade.

(3) For the cases considered the aeroelastic instability of the blade with the moment trim procedure was stronger than with the propulsive trim procedure.

(4) Coupled flap-lag behavior in forward flight seems to be relatively insensitive to precone, indicating a similarity to the effect of precone on coupled flap-lag behavior in hover.

Acknowledgment

This work was supported by Langley Directorate, U.S. Army Air Mobility Research and Development Laboratory and NASA Langley Research Center, Hampton, Virginia, under NASA NGR 05-007-414.

References

1. Y. Shulman, Stability of a flexible helicopter rotor in forward flight. J. of Aeronautical Sciences, 23, 663-670, 693 (1956).

2. G.J. Sissingh, Dynamics of rotors operating at high advance ratios. J. of the American Helicopter Society, 13, 56-63 (1968).

3. O.J. Lowis, The stability of rotor blade flapping motion at high tip speed ratios, R&M No. 3544, (1968).

4. D.A. Peters and K.H. Hohenemser, Application of the Floquet transition matrix to problems of lifting rotor stability, J. of the American Helicopter Society, 17, 3-12 (1972).

5. W.E. Hall, Application of Floquet theory to the analysis of rotary wing VTOL stability, Stanford University SUDAAR No. 400, (1970).

6. M.I. Young, A theory of rotor blade motion stability in powered flight, J. of the American Helicopter Society, 9, 12-25 (1964).

7. P. Friedmann and P. Tong, Dynamic nonlinear elastic stability of helicopter rotor blades in hover and in forward flight, NASA CR-114485, (1972).

8. P. Friedmann and P. Tong, Non-linear flap-lag dynamics of hingeless helicopter blades in hover and in forward flight, J. of Sound and Vibration, 30, 9-31 (1973).

9. P. Friedmann and L.J. Silverthorn, Aeroelastic stability of periodic systems with application to rotor blade flutter, American Institute of Aeronautics and Astronautics J., 12, 1559-1565 (1974).

10. P. Friedmann and L.J. Silverthorn, Aeroelastic stability of coupled flap-lag motion of hingeless helicopter blades at arbitrary advance ratios, J. of Sound and Vibration, 39(4), 409-428 (1975). (Also NASA CR-132431, Feb. 1974, same title.)

11. P. Friedmann, Influence of structural damping, preconing, offsets and large deflections on the flap-lag-torsional stability of a cantilevered rotor blade, AIAA Paper No. 75-780, Presented at the AIAA/ASME/SAE 16th Structures, Structural Dynamics, and Materials Conference, May 1975.

12. J.C. Houbolt and G.W. Brooks, Differential equations of motion for combined flapwise bending, chordwise bending, and torsion of twisted nonuniform rotor blades, NACA Report 1346, 1958.

13. A.R.S. Bramwell, A method for calculating the stability and control derivatives of helicopters with hingeless rotors, Research Memorandum Aero 69/4, The City University, London, 1969.

14. R.W. Brockett, Finite Dimensional Linear Systems, New York: John Wiley and Sons, 1970.

Appendix A: Definitions of the Generalized Masses, Structural and Aerodynamic Integrals and Other Quantities

The quantities $\bar{M}_{F1}$, $\bar{M}_{L1}$, $\bar{P}_{111}$, I_b, can be found in Reference 10, various other similar quantities are given below:

$$\bar{\bar{B}}^2 = \ell^3 \int_o^1 m\gamma_1\eta_1 d\bar{x}_o/I_b$$

$$\bar{B}^1 = \ell^3 \int_o^1 m(\bar{x}_o + \bar{e}_1)\eta_1 dx_o/I_b; \qquad \bar{B}^2 = \ell^3 \int_o^1 m\eta_1\gamma_1 d\bar{x}_o/I_b$$

$$\bar{P}_{111} = \ell^3 \int_o^1 (\eta_1')^2 \left[\int_{\bar{x}_o}^1 m\gamma_1 d\bar{x}_1\right] d\bar{x}_o/I_b \; ; \; \bar{\bar{P}}_{111} = \ell^3 \int_o^1 (\gamma_1')^2 \left[\int_{\bar{x}_o}^1 m\gamma_1 d\bar{x}_1\right] d\bar{x}_o/I_b$$

$$\bar{M}_{111} = \ell^3 \int_o^1 m\gamma_1 \left[\int_o^{\bar{x}_o} (\eta_1')^2 d\bar{x}_1\right] d\bar{x}_o/I_b; \; \bar{\bar{M}}_{111} = \ell^3 \int_o^1 m\gamma_1 \left[\int_{\bar{x}_o}^1 (\gamma_1')^2 d\bar{x}_1\right] d\bar{x}_o/I_b$$

$$\eta_{SF1} = \ell^3 g_{SF1} \int_o^1 \eta_1^2 \, d\bar{x}_o/(\Omega I_b 2\bar{\omega}_{F1}\bar{M}_{F1})$$

$$\eta_{SL1} = \ell^3 g_{SL1} \int_o^1 \gamma_1^2 \, d\bar{x}_o/(\Omega I_b 2\bar{\omega}_{L1}\bar{M}_{L1})$$

The structural integrals associated with elastic coupling are given by

$$E^o = [(EI)_z - (EI)_y]/2; \qquad E^s = [(EI)_z - (EI)_y] \sin 2\theta_o/2$$

$$E^c = [(EI)_z - (EI)_y] \cos 2\theta_o/2$$

$$\bar{E} = \int_o^1 E^o(\eta_1'')^2 \, d\bar{x}_o/(\ell\Omega^2 I_b) \quad ; \quad \bar{\bar{E}} = \int_o^1 E^o(\gamma_1'')^2 d\bar{x}_o/(\Omega^2 I_b \ell)$$

$$\bar{E}^c = \int_o^1 E^c(\eta_1'')^2 \, d\bar{x}_o/(\ell\Omega^2 I_b) \quad ; \quad \bar{\bar{E}}^c = \int_o^1 E^c(\gamma_1'')^2 d\bar{x}_o/(\Omega^2 I_b \ell)$$

$$\bar{E}^s = \int_o^1 E^s(\eta_1'')^2 \, d\bar{x}_o/(\ell\Omega^2 I_b) \quad ; \quad \bar{\bar{E}}^s = \int_o^1 E^s(\gamma_1'')^2 d\bar{x}_o/(\Omega^2 I_b \ell)$$

$$\bar{E}^{ls} = \int_o^1 E^s\eta_1''\gamma_1'' \, d\bar{x}_o/(\ell\Omega^2 I_b) \quad ; \quad \bar{\bar{E}}^{ls} = \int_o^1 E^s\gamma_1''\eta_1'' \, d\bar{x}_o/(\Omega^2 I_b \ell)$$

$$\bar{E}^{lc} = \int_o^1 E^c\eta_1''\gamma_1'' \, d\bar{x}_o/(\ell\Omega^2 I_b) \quad ; \quad \bar{\bar{E}}^{lc} = \int_o^1 E^c\gamma_1''\eta_1'' \, d\bar{x}_o/(\Omega^2 I_b \ell)$$

The generalized aerodynamic integrals F^i and L^i, associated with the flap and lag generalized aerodynamic loads respectively are given below. These integrals are evaluated between the lower limit $\bar{A}$ and the upper limit $\bar{B}$, where $\bar{A}$ and $\bar{B}$ are nondimensionalized tip loss factors, also

$$\bar{x}_o + \bar{e}_1 = \bar{x}$$

$$F^1 = \int \eta_1 \bar{x}^2 \, d\bar{x}_o \quad ; \quad F^2 = \int \eta_1 \bar{x} \, d\bar{x}_o \quad ; \quad F^3 = \int \eta_1 \, d\bar{x}_o$$

$$F^4 = \int \eta_1 \gamma_1' \, d\bar{x}_o \quad ; \quad F^5 = \int \eta_1 \gamma_1' \bar{x} \, d\bar{x}_o \quad ; \quad F^6 = \int \eta_1 \eta_1' \bar{x} \, d\bar{x}_o$$

$$F^7 = \int \eta_1 \eta_1' \, d\bar{x}_o \quad ; \quad F^8 = \int \eta_1^2 \bar{x} \, d\bar{x}_o \quad ; \quad F^9 = \int \eta_1^2 \, d\bar{x}_o$$

$$F^{10} = \int \eta_1 \gamma_1 \bar{x} \, d\bar{x}_o \quad ; \quad F^{11} = \int \eta_1 \gamma_1 \, d\bar{x}_o \quad ; \quad F^{12} = \int \eta_1^2 \gamma_1' \, d\bar{x}_o$$

$$F^{13} = \int \eta_1^2 \gamma_1 \, d\bar{x}_o \quad ; \quad F^{14} = \int \eta_1 \eta_1' \gamma_1 \, d\bar{x}_o \quad ; \quad F^{15} = \int \eta_1 \eta_1' \gamma_1' \, d\bar{x}_o$$

$$F^{16} = \int \eta_1 \gamma_1 \eta_1' \bar{x} d\bar{x}_o \quad ; \quad F^{17} = \int \bar{x} d\bar{x}_o \quad ; \quad F^{18} = \int \bar{x}^2 d\bar{x}_o$$

$$F^{20} = \int \bar{x} (\eta_1')^2 d\bar{x}_o \quad ; \quad F^{21} = \int d\bar{x}_o$$

$$L^1 = \int \gamma_1 \bar{x}^2 d\bar{x}_o \quad ; \quad L^2 = \int \gamma_1 \bar{x} d\bar{x}_o \quad ; \quad L^3 = \int \gamma_1 \, d\bar{x}_o$$

$$L^4 = \int \gamma_1 \eta_1' \, d\bar{x}_o \quad ; \quad L^5 = \int \gamma_1 \eta_1' \bar{x} d\bar{x}_o \quad ; \quad L^6 = \int \gamma_1 \gamma_1' \bar{x} d\bar{x}_o$$

$$L^7 = \int \gamma_1 \gamma_1' \, d\bar{x}_o \quad ; \quad L^8 = \int \gamma_1^2 \bar{x} d\bar{x}_o \quad ; \quad L^9 = \int \gamma_1^2 d\bar{x}_o$$

$$L^{10} = \int \gamma_1 \eta_1 \bar{x} d\bar{x}_o \quad ; \quad L^{11} = \int \gamma_1 \eta_1 d\bar{x}_o \quad ; \quad L^{12} = \int \gamma_1 \eta_1 \eta_1' d\bar{x}_o$$

$$L^{13} = \int \gamma_1 \eta_1^2 d\bar{x}_o \quad ; \quad L^{14} = \int \gamma_1 \eta_1' \eta_1 d\bar{x}_o \quad ; \quad L^{15} = \int \gamma_1 (\eta_1')^2 d\bar{x}_o$$

$$L^{16} = \int \gamma_1^2 \eta_1' \bar{x} d\bar{x}_o \quad ; \quad L^{17} = \int \gamma_1 \eta_1' \bar{x}^2 d\bar{x}_o \quad ; \quad L^{18} = \int \gamma_1^2 \eta_1' d\bar{x}_o$$

$$L^{19} = \int \gamma_1 \eta_1 \gamma_1' d\bar{x}_o \quad ; \quad L^{20} = \int \gamma_1^2 \eta_1 d\bar{x}_o \quad ; \quad L^{21} = \int \gamma_1 \eta_1' \gamma_1' d\bar{x}_o$$

Various other quantities needed from the trim procedure are defined below:

$$b_1 = \frac{\gamma}{2} \left(\frac{\ell}{R} \right)^2 \frac{1}{\bar{\omega}_{F1}^2 \bar{M}_{F1}} \left[F^1 + F^3 \frac{\mu^2}{2} - \frac{2\mu^2 (F^2)^2}{F^1 + 3F^3 \mu^2/4} \right]$$

$$b_2 = \frac{\gamma}{2} \left(\frac{\ell}{R} \right)^2 \frac{1}{\bar{\omega}_{F1}^2 \bar{M}_{F1}} \left[\frac{\mu^2 F^2 F^3}{F^1 + 3F^3 \mu^2/4} - F^2 \right]$$

Appendix B: Elements of the [S] and {C} Matrices

The elements of the [S] and {C} matrices required for calculating $\{q_o\}^T = \left[g_1^o,\ g_{1c},\ g_{1s},\ h_1^o,\ h_{1c},\ h_{1s}\right]$ are given below

$$S_{11} = \bar{M}_{F1}\bar{\omega}_{F1}^2 + \bar{E} - \bar{E}^c \qquad ; \qquad S_{12} = \theta_{1c}\bar{E}^s - \frac{\gamma}{4}\left(\frac{\ell}{R}\right)^3 \mu(F^9 - F^6)$$

$$S_{13} = -\theta_{1s}\bar{E}^s \quad ; \quad S_{14} = -\bar{E}^{1s} - \frac{\gamma}{2}\left(\frac{\ell}{R}\right)^4\left[\beta_p F^{10} + \frac{\mu^2}{2}\left(\frac{R}{\ell}\right)^2\beta_p F^4 - \mu\,\frac{R}{\ell}\,F^5\theta_{1c}\right]$$

$$S_{15} = -\theta_{1c}\bar{E}^{1c} - \frac{\gamma}{2}\left(\frac{\ell}{R}\right)^4\left[F^{10}\theta_{1s} + \mu\,\frac{R}{\ell}\,F^{11}\theta_o - \mu\,\frac{R}{\ell}\,F^5\theta_o + \frac{1}{2}\,\mu\left(\frac{R}{\ell}\right)^2\lambda F^4 - \frac{\mu^2}{8}\left(\frac{R}{\ell}\right)^2 F^4\theta_{1s}\right]$$

$$S_{16} = \theta_{1s}\bar{E}^{1c} - \frac{\gamma}{2}\left(\frac{\ell}{R}\right)^4\left[\mu\,\frac{R}{\ell}\,\beta_p F^{11} - F^{10}\theta_{1c} - \frac{\mu^2}{8}\left(\frac{R}{\ell}\right)^2 F^4\theta_{1c}\right]$$

$$S_{21} = 2\theta_{1c}\bar{E}^s + \frac{\gamma}{2}\left(\frac{\ell}{R}\right)^2 \mu\, F^6 \qquad ; \qquad S_{22} = \bar{M}_{F1}(\bar{\omega}_{F1}^2 - 1) + \bar{E} - \bar{E}^c$$

$$S_{23} = 2\bar{M}_{F1}\eta_{SF1}\bar{\omega}_{F1} + \frac{\gamma}{2}\left(\frac{\ell}{R}\right)^4\left[F^8 + \frac{\mu^2}{4}\left(\frac{R}{\ell}\right)^2 F^7\right]$$

$$S_{24} = -2\theta_{1c}\bar{E}^{1c} - \frac{\gamma}{2}\left(\frac{\ell}{R}\right)^4\left[-2\mu\,\frac{R}{\ell}\,F^5\theta_o + \left(\frac{R}{\ell}\right)^2\lambda\mu F^4 - \frac{\mu^2}{4}\left(\frac{R}{\ell}\right)^2 F^4\theta_{1s}\right]$$

$$S_{25} = -\bar{E}^{1s} - \frac{\gamma}{2}\left(\frac{\ell}{R}\right)^4\left[\beta_p F^{10} + 3\,\frac{\mu^2}{4}\left(\frac{R}{\ell}\right)^2\beta_p F^4 + \mu\left(\frac{R}{\ell}\right)F^{11}\theta_{1c} - 3\,\frac{\mu}{2}\,\frac{R}{\ell}\,F^5\theta_{1c}\right]$$

$$S_{26} = -2\beta_p\bar{B}^2 - \frac{\gamma}{2}\left(\frac{\ell}{R}\right)^4\left[-2F^{10}\theta_o + \frac{R}{\ell}\,F^{11}\,\lambda - \frac{\mu}{2}\left(\frac{R}{\ell}\right)F^{11}\theta_{1s} - \frac{\mu}{2}\,\frac{R}{\ell}\,F^5\theta_{1s} - \frac{\mu^2}{4}\left(\frac{R}{\ell}\right)^2 F^4\theta_o\right]$$

$$S_{31} = 2\theta_{1s}\bar{E}^s$$

$$S_{32} = -2\bar{M}_{F1}\bar{\omega}_{F1}\eta_{SF1} - \frac{\gamma}{2}\left(\frac{\ell}{R}\right)^4\left[F^8 - \frac{\mu^2}{4}\left(\frac{R}{\ell}\right)^2 F^7\right]$$

$$S_{33} = \bar{M}_{F1}(\bar{\omega}_{F1}^2 - 1) + \bar{E} - \bar{E}^c$$

$$S_{34} = -2\theta_{1s}\bar{E}^{1c} - \frac{\gamma}{2}\left(\frac{\ell}{R}\right)^4\left[\mu\,\frac{R}{\ell}\,\beta_p F^{11} - \frac{\mu^2}{4}\left(\frac{R}{\ell}\right)^2 F^4\theta_{1c}\right]$$

$$S_{35} = 2\beta_p\bar{B}^2 - \frac{\gamma}{2}\left(\frac{\ell}{R}\right)^4\left[2F^{10}\theta_o - \frac{R}{\ell}\,F^{11}\,\lambda + \frac{3}{2}\,\mu\,\frac{R}{\ell}\,F^{11}\theta_{1s} - \frac{\mu}{2}\,\frac{R}{\ell}\,F^5\theta_{1s} - \frac{\mu^2}{4}\left(\frac{R}{\ell}\right)^2 F^4\theta_o\right]$$

$$S_{36} = -\bar{E}^{1s} - \frac{\gamma}{2}\left(\frac{\ell}{R}\right)^4\left[\beta_p F^{10} + \frac{\mu^2}{4}\left(\frac{R}{\ell}\right)^2\beta_p F^4 - \frac{\mu}{2}\,\frac{R}{\ell}\,F^{11}\theta_{1c} - \frac{\mu}{2}\left(\frac{R}{\ell}\right)F^5\theta_{1c}\right]$$

$$S_{41} = \bar{\bar{E}}^{1s} + \frac{\gamma}{2}\left(\frac{\ell}{R}\right)^4\left[-\mu^2\left(\frac{R}{\ell}\right)^2\beta_p L^4 + \frac{\mu}{2}\left(\frac{R}{\ell}\right)L^5\theta_{1c}\right]$$

$$S_{42} = \bar{\bar{E}}^{1c}\theta_{1c} + \frac{\gamma}{2}\left(\frac{\ell}{R}\right)^4\left[-\frac{1}{2}\,L^{10}\theta_{1s} + \frac{\mu}{2}\,\frac{R}{\ell}\,\theta_o L^5 - \frac{\mu}{2}\,\frac{R}{\ell}\,\theta_o L^{11} - \mu\left(\frac{R}{\ell}\right)^2\lambda L^4 + \frac{\mu^2}{8}\left(\frac{R}{\ell}\right)^2 L^4\theta_{1s}\right]$$

$$S_{43} = \bar{\bar{E}}^{1c}\theta_{1s} + \frac{\gamma}{2}\left(\frac{\ell}{R}\right)^4\left[\frac{1}{2}\,L^{10}\theta_{1c} - \mu\,\frac{R}{\ell}\,\beta_p L^{11} + \frac{\mu^2}{8}\left(\frac{R}{\ell}\right)^2 L^4\theta_{1c}\right]$$

$$S_{44} = -\bar{\bar{\omega}}_{L1}^{2}\,\bar{\bar{M}}_{L1} + (\bar{\bar{E}} - \bar{\bar{E}}^{c}) - (\gamma/2)(\ell/R)^{4}\,\beta_p\theta_o L^8$$

$$S_{45} = \bar{\bar{E}}^{s}\theta_{1c} + (\gamma/2)(\ell/R)^{4}\mu(Cdo/a)(R/\ell)L^9$$

$$S_{46} = -(\gamma/4)(\ell/R)^{3}\mu\beta_p\theta_o L^9 + \bar{\bar{E}}^{s}\theta_{1s}$$

$$S_{51} = 2\,\bar{\bar{E}}^{1c}\theta_{1c} + (\gamma/2)(\ell/R)^{3}\,[\mu\theta_o L^5 - 2\mu(R/\ell)\lambda L^4 + (\mu^2/4)(R/\ell)L^4\theta_{1s})$$

$$S_{52} = \bar{\bar{E}}^{1s} + (\gamma/2)(\ell/R)^{3}\,[-\mu^2(R/\ell)(1.5)\beta_p L^4 + 0.75\,L^5\theta_{1c}\mu - 0.25\,L^{11}\theta_{1c}]$$

$$S_{53} = 0.5\gamma(\ell/R)^{4}\,[L^{10}\theta_o - 2(R/\ell)\lambda L^{11} + 0.25(R/\ell)(L^5 + L^{11})\mu\theta_{1s} + 0.25(R/\ell)\mu^2\theta_o L^4] - 2\beta_p\,\bar{\bar{B}}^{2}$$

$$S_{54} = 2\,\bar{\bar{E}}^{s}\theta_{1c} \quad ; \quad S_{55} = \bar{\bar{M}}_{L1}(1-\bar{\bar{\omega}}_{L1}^{2}) + (\bar{\bar{E}} - \bar{\bar{E}}^{c}) - (\gamma/2)(\ell/R)^{4}\beta_p\theta_o L^8$$

$$S_{56} = -2\bar{\bar{M}}_{L1}\,\bar{\bar{\omega}}_{L1}\eta_{SL1} - (\gamma/2)(\ell/R)^{4}\,[\,2Cdo\,L^8/a + (R/\ell)\lambda\theta_o L^9]$$

$$S_{61} = 2\,\bar{\bar{E}}^{1c}\theta_{1s} + (\gamma/8)(\ell/R)^{2}L^4\theta_{1c}\mu^2$$

$$S_{62} = (\gamma/2)(\ell/R)^{4}\,[-L^{10}\theta_o + 2(R/\ell)\lambda L^{11} + 0.25(R/\ell)L^5\theta_{1s} - 0.75\mu\,(R/\ell)L^{11}\theta_{1s} + 0.25\mu^2(R/\ell)^2\theta_o L^4] + 2\,\beta_p\bar{\bar{B}}^{2}$$

$$S_{63} = \bar{\bar{E}}^{1s} + (\gamma/2)(\ell/R)^{3}\,[-\mu^2(R/\ell)\beta_p L^4 + 0.25(L^5 + L^{11})\mu\theta_{1c} + 0.5\mu^2(R/\ell)L^4\beta_p]$$

$$S_{64} = 2\theta_{1s}\bar{\bar{E}}^{s} \quad ; \quad S_{65} = 2\bar{\bar{M}}_{L1}\bar{\bar{\omega}}_{L1}\eta_{SL1} + (\gamma/2)(\ell/R)^{4}\,[2\,Cdo\,L^8/a + (R/\ell)\lambda\theta_o L^9]$$

$$S_{66} = \bar{\bar{M}}_{L1}(1-\bar{\bar{\omega}}_{L1}^{2}) + (\bar{\bar{E}} - \bar{\bar{E}}^{c}) - (\gamma/2)(\ell/R)^{4}\beta_p\theta_o L^8$$

$$C_1 = (\gamma/2)(\ell/R)^{4}\,[F^1\theta_o + 0.5\,(R/\ell)^2\mu^2F^3\theta_o - (R/\ell)\lambda F^2 + \mu(R/\ell)F^2\theta_{1s} - 0.75\mu b(R/\ell)^2\theta_{1c}F^3] - \beta_p\bar{\bar{B}}^{1}$$

$$C_2 = (\gamma/2)(\ell/R)^{4}[F^1\theta_{1c} + 0.25\mu^2(R/\ell)^2F^3\theta_{1c} + 1.5\,b(R/\ell)\theta_{1s}F^2 - \mu(R/\ell)\beta_p F^2]$$

$$C_3 = (\gamma/2)(\ell/R)^{4}\,[F^1\theta_{1s} + 2\mu(R/\ell)F^2\theta_o + 0.5(R/\ell)^2\mu^2F^3\theta_{1s} - 1.5\,b(R/\ell)F^2\theta_{1c} - \mu(R/\ell)^2\,\lambda F^3 + 0.25\,\mu^2(R/\ell)^2F^3\theta_{1s}]$$

$$C_4 = -(\gamma/2)(\ell/R)^4 \Big\{ \lambda(R/\ell)L^2\theta_o - (R/\ell)^2\lambda^2 L^3 - 0.5\,\mu^2(R/\ell)^2\beta_p^2\,L^3$$
$$+ (Cdo/a)[L^1 + 0.5\,\mu^2(R/\ell)^2 L^3] + 0.5\,\mu(R/\ell)\beta_p L^2\theta_{1c} + 0.5(R/\ell)^2\mu\lambda L^3\theta_{1s} \Big\}$$

$$C_5 = -0.5\gamma(\ell/R)^4\,[(R/\ell)\lambda L^2\theta_{1s} + \mu(R/\ell)\beta_p L^2\theta_o - 2\mu(R/\ell)^2\lambda\beta_p L^3 + 0.25\mu^2(R/\ell)^2\beta_p L^3\theta_{1s}]$$

$$C_6 = -0.5\gamma(\ell/R)^3\,[\,\lambda\,L^2\theta_{1s} + \mu(R/\ell)\lambda\theta_o L^3 + 2(Cdo/a)\mu L^2 + 0.25\mu^2(R/\ell)\beta_p L^3\theta_{1c}]$$

Appendix C: Elements of the [A]-Matrix

The elements of the [A]-matrix, which define the equations of motion when written as a set of first order differential equations in state variable form, are given below:

$$A_{21} = 1,\ A_{22} = A_{23} = A_{24} = 0,\ A_{43} = 1,\ A_{41} = A_{42} = A_{44} = 0$$

$$A_{11} = -2\,\bar{\omega}_{F1}\eta_{SF1} - (1/M_{F1})(\gamma/2)(\ell/R)^4\Big[F^8 - \mu(R/\ell)F^{12}\bar{h}_1\cos\psi - F^{13}\,\bar{\bar{h}}_1 + \mu(R/\ell)F^9\sin\psi\Big]$$

$$A_{12} = -\bar{\omega}_{F1}^2 - (1/M_{F1})\Big\{ -2\,\bar{\bar{h}}_1\bar{P}_{111} + \bar{E} - \bar{E}^c\cos2\theta_t + \bar{E}^s\sin2\theta_t + (\gamma/2)(\ell/R)^4\Big[-F^{16}\,\bar{h}_1$$
$$+ \mu(R/\ell)F^6\cos\psi - \mu(R/\ell)F^{14}\,\bar{\bar{h}}_1\cos\psi - \mu(R/\ell)F^{14}\,\bar{h}_1\sin\psi + (\mu^2/2)(R/\ell)^2F^7\sin2\psi$$
$$- (\mu^2/2)(R/\ell)^2F^{15}\,\bar{h}_1(1 + \cos2\psi)\Big]\Big\}$$

$$A_{13} = -(1/M_{F1})\Big\{ -2\,\beta_p\bar{B}^2 - 2\,\bar{P}_{111}\bar{g}_1 + (\gamma/2)(\ell/R)^4\Big[2F^{10}(\theta_o + \theta_t)$$
$$+ 2\mu(R/\ell)F^{11}(\theta_o + \theta_t)\sin\psi - \mu(R/\ell)\beta_p F^{11}\cos\psi$$
$$- \mu(R/\ell)F^{14}\,\bar{g}_1\cos\psi - (R/\ell)\lambda\,F^{11} - F^{13}\,\bar{\bar{g}}_1\Big]\Big\}$$

$$A_{14} = -(1/M_{F1})\Big\{ -\bar{E}^{1s}\cos2\theta_t - \bar{E}^{1c}\sin2\theta_t + (\gamma/2)(\ell/R)^4\Big[2\mu(R/\ell)F^5(\theta_o + \theta_t)\cos\psi$$
$$+ \mu^2(R/\ell)^2F^4(\theta_o + \theta_t)\sin2\psi - \beta_p F^{10} - F^{16}\,\bar{g}_1$$
$$- \mu(R/\ell)^2\lambda F^4\cos\psi - \mu(R/\ell)F^{12}\,\bar{\bar{g}}_1\cos\psi$$
$$- \mu(R/\ell)\beta_p F^{11}\sin\psi - \mu(R/\ell)F^{14}\,\bar{g}_1\sin\psi$$
$$- (\mu^2/2)(R/\ell)^2\beta_p F^4(1 + \cos2\psi) - (\mu^2/2)(R/\ell)^2F^{15}\bar{g}_1(1 + \cos2\psi)\Big]\Big\}$$

$$A_{31} = -(1/M_{L1}) \left\{ 2\beta_p \bar{\bar{B}}^2 + 2\bar{M}_{111}\bar{g}_1 - (\gamma/2)(\ell/R)^4 \left[L^{10}(\theta_o + \theta_t) \right.\right.$$

$$+ \mu(R/\ell)L^{11}(\theta_o + \theta_t)\sin\psi - 2(R/\ell)\lambda L^{11} - 2\mu(R/\ell)\beta_p L^{11}\cos\psi$$

$$\left.\left. - 2\mu(R/\ell)L^{12}\bar{g}_1\cos\psi - 2\overset{*}{\bar{g}}_1 L^{13} - \theta_o L^{20}\overset{*}{\bar{h}}_1 \right] \right\}$$

$$A_{32} = -(1/M_{L1}) \left\{ 2\bar{M}_{111}\overset{*}{\bar{g}}_1 - \bar{\bar{E}}^{1s}\cos 2\theta_t - \bar{\bar{E}}^{1c}\sin 2\theta_t \right.$$

$$- (\gamma/2)(\ell/R)^4 \left[\mu(R/\ell)L^5(\theta_o + \theta_t)\cos\psi + (\mu^2/2)(R/\ell)^2 L^4(\theta_o + \theta_t)\sin 2\psi \right.$$

$$- 2\mu(R/\ell)^2\lambda L^4\cos\psi - 2\mu(R/\ell)L^{12}\overset{*}{\bar{g}}_1\cos\psi$$

$$- \mu^2(R/\ell)^2\beta_p L^4(1 + \cos 2\psi) - \mu^2(R/\ell)^2 L^{15}\bar{g}_1(1 + \cos 2\psi)$$

$$\left.\left. - \mu(R/\ell)\theta_o L^{18}\overset{*}{\bar{h}}_1\cos\psi - \theta_o L^{16}\bar{h}_1 \right] \right\}$$

$$A_{33} = -2\bar{\omega}_{L1}\eta_{SL1} - (1/\bar{M}_{L1})(\gamma/2)(\ell/R)^4 \left[2(C_{do}/a)L^8 \right.$$

$$+ 2(C_{do}/a)\mu(R/\ell)L^9\sin\psi + \mu(R/\ell)\beta_p\theta_o L^9\cos\psi$$

$$\left. + \mu(R/\ell)\theta_o L^{18}\bar{g}_1\cos\psi + \theta_o L^{20}\overset{*}{\bar{g}}_1 + (R/\ell)\lambda\theta_o L^9 \right]$$

$$A_{34} = -\bar{\omega}_{L1}^2 - (1/\bar{M}_{L1}) \left\{ \bar{\bar{E}}^c\cos 2\theta_t - \bar{\bar{E}}^s\sin 2\theta_t - \bar{\bar{E}} + (\gamma/2)(\ell/R)^4 [\beta_p\theta_o L^8 + \theta_o L^{16}\bar{g}_1] \right\}$$

Appendix D: List of Symbols

a	=	two dimensional lift curve slope
$\bar{A},\bar{B}$	=	tip loss coefficients
$[A]$	=	periodic matrix, with elements A_{ij}, defined in Appendix C
A_{F1},A_{L1}	=	generalized aerodynamic force for the first flap and lag mode, respectively
b	=	semi-chord, non-dimensionalized with respect to R
$\bar{B}^i,\bar{\bar{B}}^i$	=	generalized masses defined in Appendix A
b_1,b_2	=	coefficients defined in Appendix A
$C_T = T/\rho_A(\pi R^2\Omega^2R^2)$	=	thrust coefficient
$\{C\}$	=	constant column matrix, defined in Appendix B
C_{do}	=	profile drag coefficient
$C(k)$	=	Theodorsen's lift deficiency function
$[C]$	=	constant matrix used in Floquet-Liapunov theorem
C_H	=	$H/(\rho_A\pi R^2\Omega^2R^2)$ horizontal force coefficient
C_{DP}	=	Drag coefficient due to equivalent flat plate area of the helicopter $(f/\pi R^2)$
D_p	=	parasite drag of the helicopter
$E_{c1},E_{c2},\bar{E}^o,\bar{E}^s,\bar{E}^c$ etc.	=	terms associated with elastic coupling defined in Appendix A
$(EI)_y,(EI)_z$	=	stiffness for flapwise and inplane bending, respectively
F^i	=	aerodynamic integrals for flap equation defined in Appendix A
f	=	equivalent flat plate area of the helicopter
g_1	=	generalized coordinate, first normal flapping mode
Δg_1	=	perturbation in g_1 about $\bar{g}_1$
g_1^o	=	static value of g_1 in hover
$\tilde{g}_1^o,\tilde{g}_{1s},\tilde{g}_{1c}$	=	constant and cyclic first mode flapping coefficients evaluated from trim procedures
g_1^o	=	constant part of $\bar{g}_1$
$\bar{g}_1$	=	linear time dependent equilibrium value of first normal flapping mode
g_{1c},g_{1s}	=	cyclic parts of $\bar{g}_1$

g_{SF}, g_{SL}	=	viscous structural damping in flap and lag, respectively
h_1	=	generalized coordinate, first normal inplane mode
Δh_1	=	perturbation in h_1 about $\bar{h}_1$
h_1^o	=	constant part of $\bar{h}_1$
h_{1s}, h_{1c}	=	cyclic parts of $\bar{h}_1$
$\bar{h}_1$	=	linear time dependent equilibrium value of first normal lead lag mode
H	=	horizontal force Fig. 3
i	=	$\sqrt{-1}$
$\underset{\sim}{i}, \underset{\sim}{j}, \underset{\sim}{k}$	=	unit vectors in x,y and z direction, Fig. 1
$\underset{\sim}{I}_2, \underset{\sim}{J}_2, \underset{\sim}{K}_2$ $\underset{\sim}{I}_3, \underset{\sim}{J}_3, \underset{\sim}{K}_3$	=	unit vectors defining deformed blade geometry, shown in Fig. 2. $\underset{\sim}{J}_2$ is parallel to hub plane, $\underset{\sim}{I}_2$ and $\underset{\sim}{I}_3$ are tangential to the deformed blade elastic axis.
I_b	=	mass moment of inertia in flap, defined in Appendix A
ℓ	=	length of blade capable of elastic deflection
L^i	=	aerodynamic integrals associated with lag equation defined in Appendix A
L_{Y2}, L_{Z2}	=	aerodynamic loads per unit length in the $\underset{\sim}{J}_2$ and $\underset{\sim}{K}_2$ directions respectively, approximately coincident with $\underset{\sim}{j}$, and $\underset{\sim}{k}$ directions
$(M_{pa})_R, (M_{ra})_R$	=	average pitching and rolling moment for the complete rotor
M_{pa}, M_{ra}	=	average pitching and rolling moment for a single blade
m	=	mass of blade per unit length
m_A	=	total mass of the aircraft
$\bar{M}_{Fl}, \bar{M}_{Ll}$	=	generalized masses for the i^{th} flap and lag modes, respectively, defined in Appendix A
$\bar{M}_{111}, \bar{\bar{M}}_{111}$	=	defined in Appendix A
M_p, M_r	=	instantaneous pitching and rolling moment
$M_R(0,\psi)$	=	total bending moment at blade root
n_b	=	number of blades
p_x, p_y, p_z	=	resultant total loadings per unit length in the x,y and z directions, respectively
$\bar{P}_{111}$	=	defined in Appendix A
$[P(\psi)]$	=	periodic matrix

$\{q_o\}$	=	vector of variables defining time dependent equilibrium position of the blade
R	=	blade radius
[R]	=	constant matrix used in Floquet-Liapunov theorem
[S]	=	matrix used in calculating equilibrium position defined in Appendix B
T	=	centrifugal tension in the blade, also common non-dimensional period used in the Floquet theory, also thrust in trim procedure
u,v,w	=	x,y and z displacements of a point on the elastic axis of the blade
$U_P, -U_{Z2}$ $U_T, -U_{Y2}$	=	relative velocity components of blade elastic axis, in the $\underset{\sim}{J}_2$ and $\underset{\sim}{K}_2$ directions
v_e, v_{eo}	=	elastic part of the displacement of a point on the elastic axis of the blade parallel to the hub plane (see Fig. 1), subscript 0 denotes equilibrium position
V	=	velocity of forward flight of the whole rotor
w_e, w_{eo}	=	elastic part of the displacement of a point on the elastic axis of the blade, in the $\underset{\sim}{K}_Z$ direction, Fig. 2, subscript o denotes equilibrium position
x,y,z	=	rotating orthogonal coordinate system
$x_o = x - e_1$	=	running spanwise coordinate for part of the blade free to deflect elastically, x_1-same, dummy variable
{y}	=	state variable column matrix
α_R	=	angle of attack of the whole rotor
β_p	=	preconing, inclination of feathering axis w.r.t. the hub plane measured in a vertical plane
γ	=	lock number ($\gamma = 2\rho_A b R^5 a / I_b$) for normal flow
γ_1	=	first inplane bending mode
$\mathscr{E}_D$	=	symbolic quantity having the same order of magnitude as the displacements v and w
ζ_k	=	real part of the k^{th} characteristic exponent
η_1	=	first flapwise bending mode
η_{SF1}, η_{SL1}	=	viscous structural damping coefficients defined in Appendix A, in percent of critical damping, for first flap and lag mode, respectively
θ_o	=	collective pitch angle

θ_G	=	total geometric pitch angle
θ_t	=	time dependent part of geometric pitch angle
θ_{lc}, θ_{ls}	=	cyclic pitch components
θ_c	=	critical value of collective pitch at which linearized coupled flap-lag system becomes unstable in hover
λ	=	inflow ratio, induced velocity over disk, positive down, non-dimensionalized w.r.t. ΩR
λ_k	=	eigenvalues of [R], characteristic exponents
μ	=	advance ratio
μ_c	=	critical value of advance ratio at which flap-lag system becomes unstable
ρ_A	=	density of air
σ	=	blade solidity ratio
$[\Phi(\psi,\psi_o)]$	=	state transition matrix at ψ, for initial conditions given at ψ_o
ψ	=	azimuth angle of blade ($\psi = \Omega t$) measured from straight aft position
ω_k	=	imaginary part of k^{th} characteristic exponent
$\bar{\omega}_{F1}, \bar{\omega}_{L1}$	=	natural frequency of first flap or lead-lag mode, rotating
Ω	=	speed of rotation

Special Symbols

$(^*)$	=	differentiation with respect to ψ
$(\bar{\ })$	=	non-dimensionalized quantity, length for elastic properties non-dimensionalized w.r.t. l; all other w.r.t. R, frequencies w.r.t. Ω; mass properties w.r.t. I_b
$()'$	=	differentiation w.r.t. $\bar{x}_o$
$(\sim)$	=	the symbol ~ beneath a quantity denotes a vector

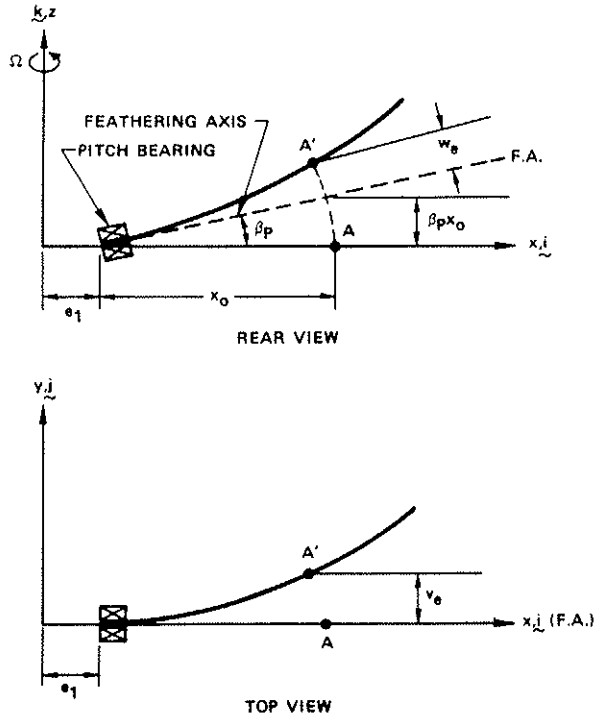

Figure 1 Deformed Elastic Axis for a Cantilevered, Preconed Rotor Blade.

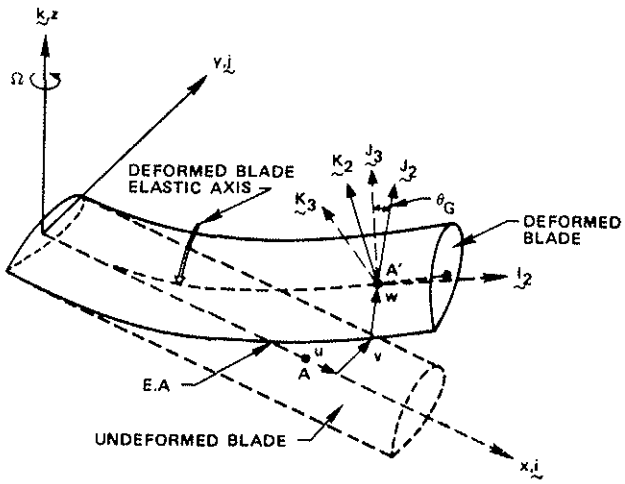

Figure 2. Schematic Representation of Deformed and Undeformed Blade.

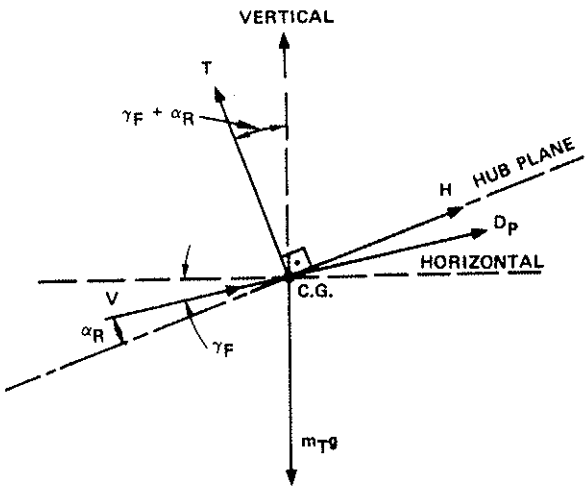

Figure 3. Geometry for Trim Calculation.

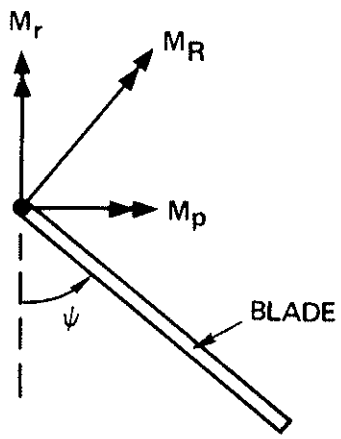

Figure 4. Blade Root Moment Decomposition

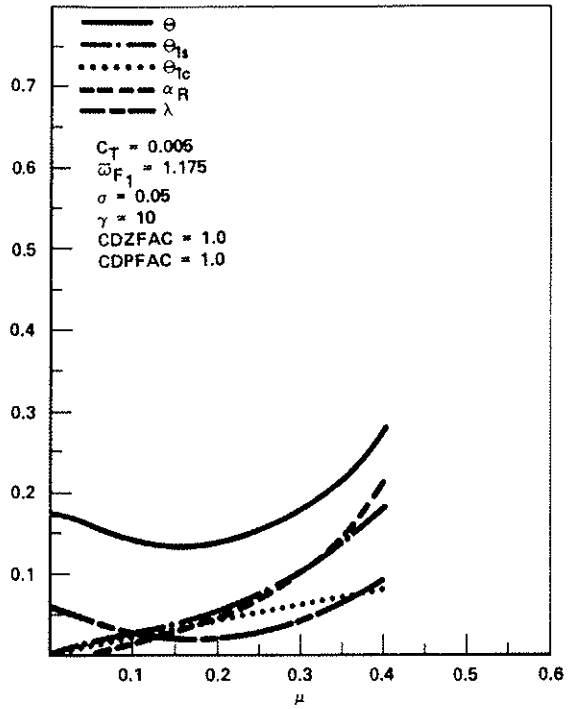

Figure 5. Typical Propulsive Trim Curves for $C_T = 0.005$.

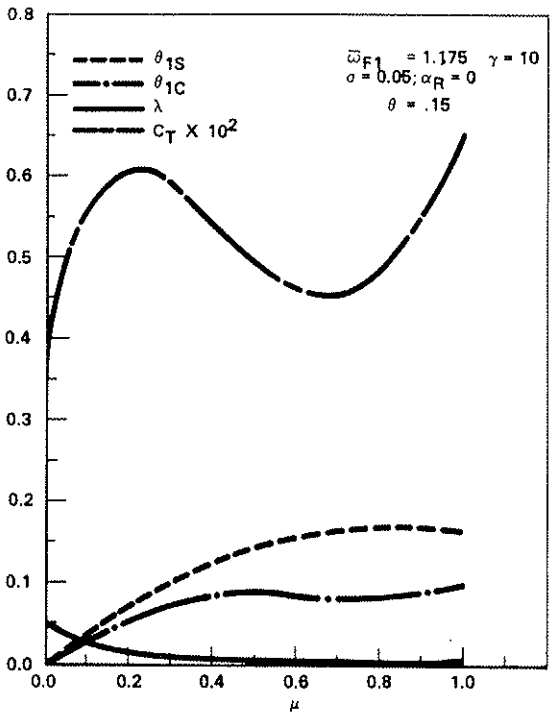

Figure 6. Typical Trim Curves for Moment Trim.

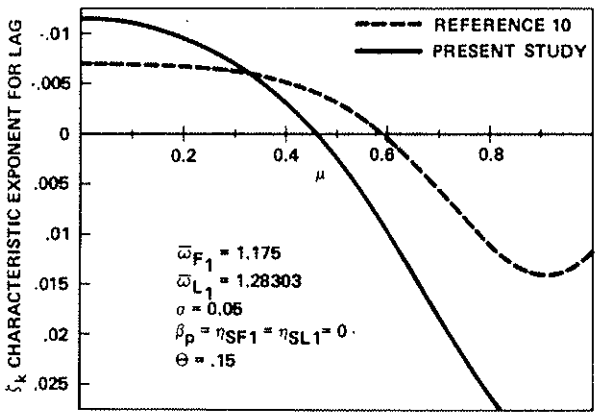

Figure 7. Effect of Correction Terms on Previous Results for a Typical Case.

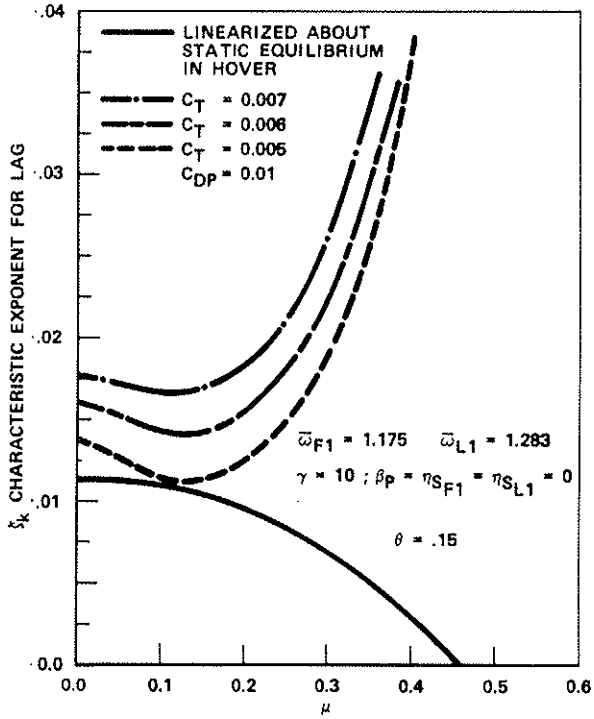

Figure 8. Effect of Propulsive Trim on a Typical Case.

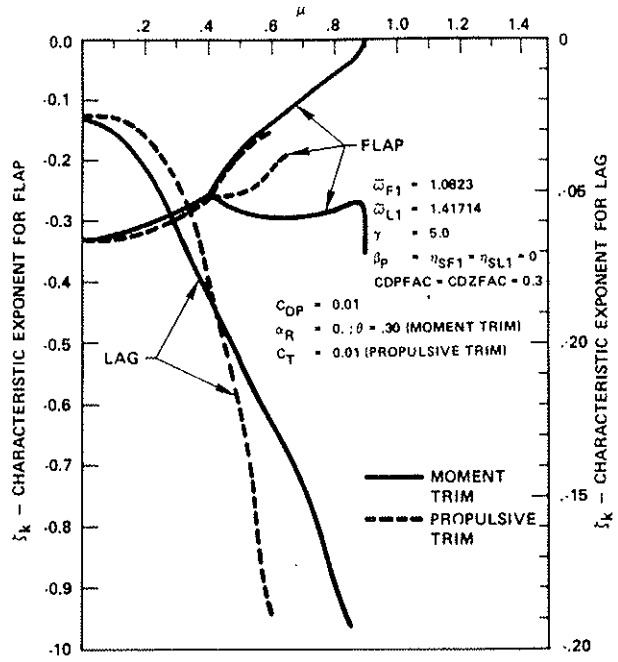

Figure 9. Combined Effect of Trim Procedures and Lock Number on Blade Stability.

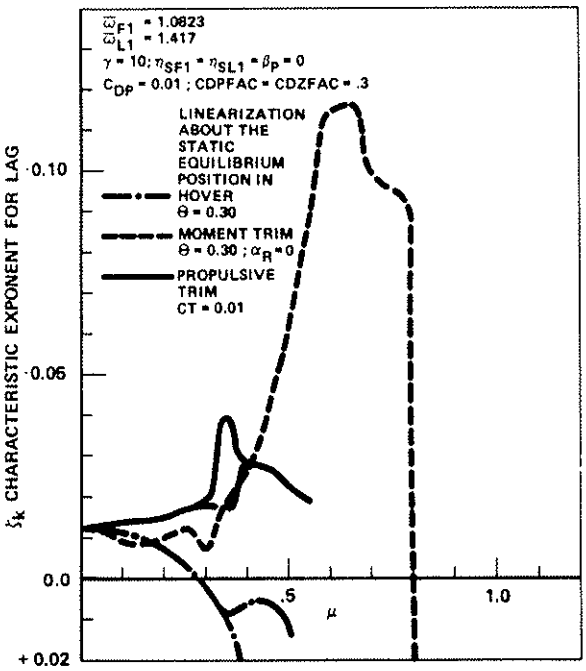

Figure 10. Combined Effect of Trim Procedures and Lock Number on Blade Stability.

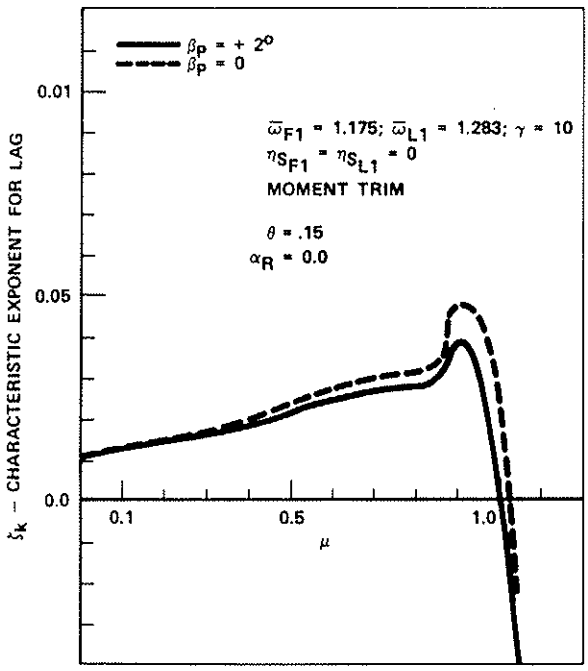

Figure 11. Effect of Rotor Angle of Attack α_R.

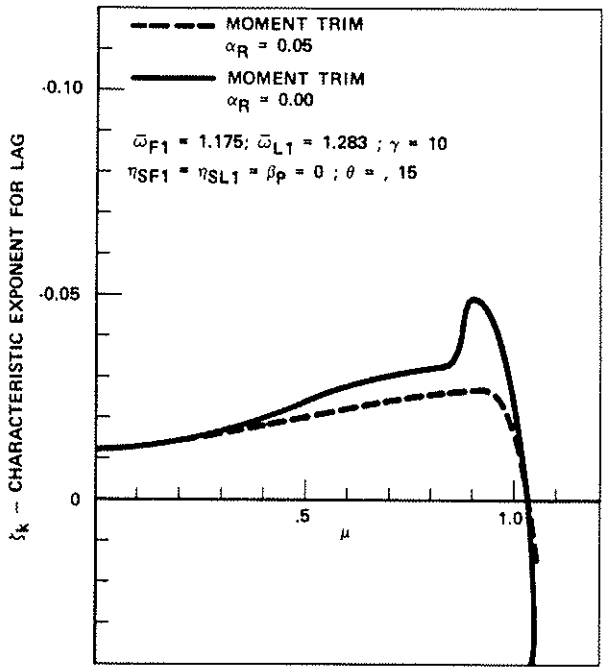

Figure 12. Effect of Precone on Blade Stability.

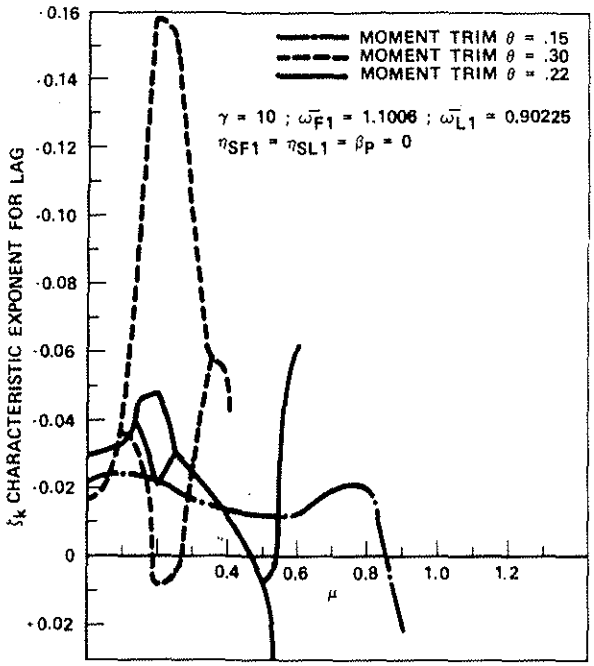

Figure 13. Effect of Moment Trim on a Soft Inplane Blade.

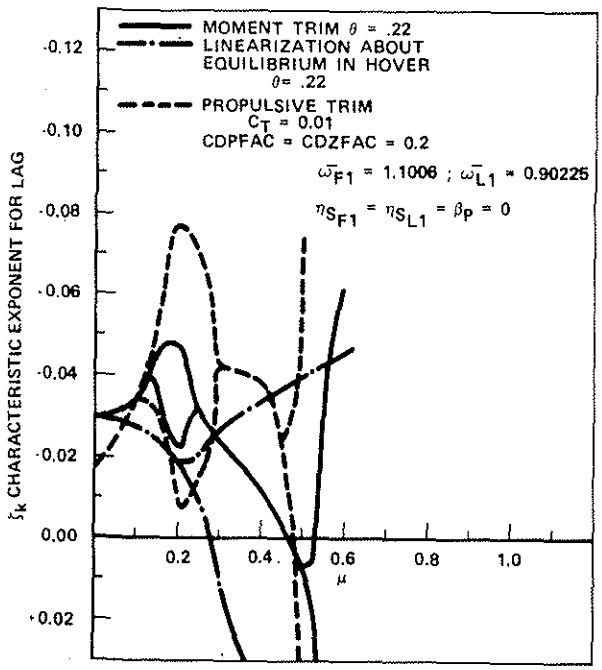

Figure 14. Effect of Propulsive and Moment Trim on a Soft In-Plane Blade.